

## **PROJECT 1.1: DETECTION AND ATTRIBUTION OF CHANGES TO WEATHER SYSTEMS AND LARGE SCALE CIRCULATION DRIVERS**

### **Principal Investigators**

*Carsten Segerlund Frederiksen*, Bureau of Meteorology, Centre for Australian Weather and Climate Research, PO Box 1289, Melbourne, Victoria, 3001  
Phone: 03 9669 4566; Email: [c.frederiksen@bom.gov.au](mailto:c.frederiksen@bom.gov.au)

*Jorgen Segerlund Frederiksen*, CSIRO Marine and Atmospheric Research, Centre for Australian Weather and Climate Research, Private Bag 1, Aspendale, Victoria, 3195, Phone: 03 92394683; Email: [jorgen.frederiksen@bom.gov.au](mailto:jorgen.frederiksen@bom.gov.au)

### **Senior Investigator**

*Meelis Zidikheri*, Bureau of Meteorology, Centre for Australian Weather and Climate Research, PO Box 1289, Melbourne, Victoria, 3001  
Phone: 03 9669 4427; Email: [m.zidikheri@bom.gov.au](mailto:m.zidikheri@bom.gov.au)

### **Objectives**

- To use observational methods and dynamical models to study the changes in the observed mean climate of the SH circulation and high frequency weather systems affecting the climates of the South-West and North-West in all seasons.
- To study changes in the SH mean climate and transients within climate models forced by observed anthropogenic forcing.
- To study the observed changes in low frequency weather systems affecting the South-West and North-West and compare with climate models under anthropogenic climate forcing.
- To analyse projections of changes in SH circulation and WA weather systems under different future IPCC scenarios.
- To formulate and develop an inverse modelling technique to identify a “fingerprint” of climate change forcing in each season.
- To produce a “fingerprint” of climate change forcing associated with observed changes in the mean SH climate and WA weather systems.
- To attribute the causes of observed changes in WA weather systems.

### **Key Research Findings**

- The changes in Southern Hemisphere autumn and winter storms have been studied using a global two-level primitive equation instability model with reanalysed observed May and July basic states during the 20th century.
- For July, storm track modes growing on the subtropical jet show a dramatic reduction in growth rate post-1975. This reduction in the intensity of storm development has continued to the present time for storm track modes that cross Australia and is associated with the observed decrease in rainfall in southwest Australia (SWWA).
- For May, the strength of the subtropical storm track crossing Australia has decreased while the polar storm track has increased. This again is associated with a decrease in the strength of the divergence field and rainfall over SWWA and generally across southern Australia. These effects have become more pronounced with time.
- For both autumn and winter, the rainfall reduction is also associated with a decrease in the vertical mean latitudinal temperature gradient and in the peak upper tropospheric jet-stream zonal winds near 30° south throughout most of the Southern Hemisphere.
- The performance of coupled models to simulate twentieth century winter circulation changes throughout the southern hemisphere, and particularly over Australia has been examined. Changes include a decrease in the vertical mean meridional temperature gradient and in the peak upper tropospheric jet-stream zonal winds throughout most of the southern hemisphere, but especially upstream and over Australia. These and other circulation changes, including changes in the Hadley circulation, and trends in the Southern Annular Mode, affect winter rainfall over SWWA and southern Australia.
- The response of the Coupled Model Intercomparison Project 3 (CMIP3) climate models to observed anthropogenic forcing, including increasing greenhouse gases, from pre-industrial to the end of the twentieth century has been examined and compared with reanalysed observations. Focus has been on the ability to simulate (a) the reduction in the strength of the wintertime subtropical 300hPa zonal wind upstream and over southern Australia, and a

strengthening in the zonal wind further south, and (b) a reduction in the baroclinic instability, related to the vertical wind shear, of the subtropical SH circulation.

- The CMIP3 models display quite disparate abilities to simulate these two diagnostics. Our analysis also suggests that there is a component of decadal variability in the model results that is dependent on the base period chosen in the pre-industrial runs.
- The better CMIP3 models suggest that further large reductions in the growth rate of storm track modes affecting SWWA, as well as rainfall, are possible under SRESB1, SRESA1B and SRESA2 scenarios, especially over the Australian region.
- The ability of a number of climate models with anthropogenic forcing, including increasing greenhouse gas concentrations, to replicate the changes in transient weather systems during the 20th century has also been examined. In particular, the CSIRO Mark 3.0 and 3.5, UKMO HAdGem1 coupled models, and the ACCESS atmospheric model, have been examined. The first 3 models have some difficulty reproducing the observed changes, but the ACCESS model reproduced the observed storm track quite well.

## **MILESTONE 1.1.1: REPORT ON OBSERVED CHANGES IN MEAN SH CLIMATE AND HIGH FREQUENCY SYSTEMS AFFECTING WA**

### **Background**

#### *Summary*

The changes in Southern Hemisphere autumn and winter storms have been studied using a global two-level primitive equation instability model with reanalysed observed May and July basic states during the 20th century. For July, storm track instability modes growing on the subtropical jet show a dramatic reduction in growth rate post-1975. This reduction in the intensity of storm development has continued to the present time for storm track modes that cross Australia and is associated with the observed decrease in rainfall in southwest Australia (SWWA). For May, the strength of the subtropical storm track crossing Australia has decreased while the polar storm track has increased. This again is associated with a decrease in the strength of the divergence field and rainfall over SWWA and generally across southern Australia. These effects have become more pronounced with time. We find for both autumn and winter that the rainfall reduction is also associated with a decrease in the vertical mean latitudinal temperature gradient and in the peak upper tropospheric jet-stream zonal winds near 30° south throughout most of the Southern Hemisphere.

#### *Introduction*

During the second half of the 20<sup>th</sup> century there have been significant reductions in the rainfall particularly across south west Western Australia (SWWA) across southern Australia and (Nicholls 2007; Bates et al. 2008; Cai and Cowan 2008; Ummenhofer et al. 2008). For this milestone, the changes in Southern Hemisphere autumn and winter storm track modes during the 20<sup>th</sup> century have been studied based on May and July reanalysed observations and on data from climate models (see milestone 1.1.2 below). Frederiksen and Frederiksen (2005, 2007) showed that there had been a dramatic reduction in the growth rates of storm track modes crossing Australia in the 1975-

1994 reanalyses. Here, we examine whether this reduction has continued into the present time. We also study the corresponding changes in autumn, focusing on the month of May.

### **Technical Details**

The global Southern Hemisphere (SH) July climates for the periods 1949-1968 and 1975-1994, using the National Centres for Environmental Prediction (NCEP) reanalyses, have been compared and there are significant differences between the two periods. Most noticeable is a reduction of about 17% in the peak strength of the SH subtropical jet stream (Figure 1 of Frederiksen and Frederiksen 2007). There have been further reductions into the period 1997-2006. Similar changes occur in May between 1949-68 and the later periods 1975-94 and 1997-2006 but with the decrease in the strength of the subtropical jet (near 30° S) being slightly less and the increase in the polar jet (near 60° S) slightly more (not shown). These changes can be expected to affect the properties of the storm track modes over southern Australia.

In both periods, there is a maximum in the zonal wind strength in the subtropics (near 30S) at about the 200hPa pressure level. This is directly associated with changes in the Hadley circulation in the Southern Hemisphere. The thermal structure of the SH atmosphere has also changed with a significant warming south of 30S, tending to reduce the equator-pole temperature gradient (not shown). Such changes would be expected to have a significant effect on the stability of the SH circulation and hence on the nature of the SH storms, which have a major impact on SWWA, and other modes of weather variability. In fact, in both July and May (not shown) the SH atmosphere has generally become less unstable in those regions associated with the generation of mid-latitude storms.

### *Changes in Storm Track Modes from Reanalyses*

An analysis of the impact of these observed SH winter climate changes on the nature of the dominant SH weather modes, was conducted, with particular emphasis on the storm track modes. Here, we have used the primitive equation instability model

described in Frederiksen and Frederiksen (2005, 2007) to identify the dominant unstable weather modes in each period. In the earlier period, the fastest growing weather mode is a SH storm mode which affects southern Australia, and has largest impact over SWWA (Figure 1.1.1). This mode consists of a series of eastward propagating troughs (blue shading) and ridges (red shading), and is shown in the top panel of Figure 1.1.1 at a particular instance. . As the troughs and ridges move eastward they amplify to reach a maximum in preferred regions.

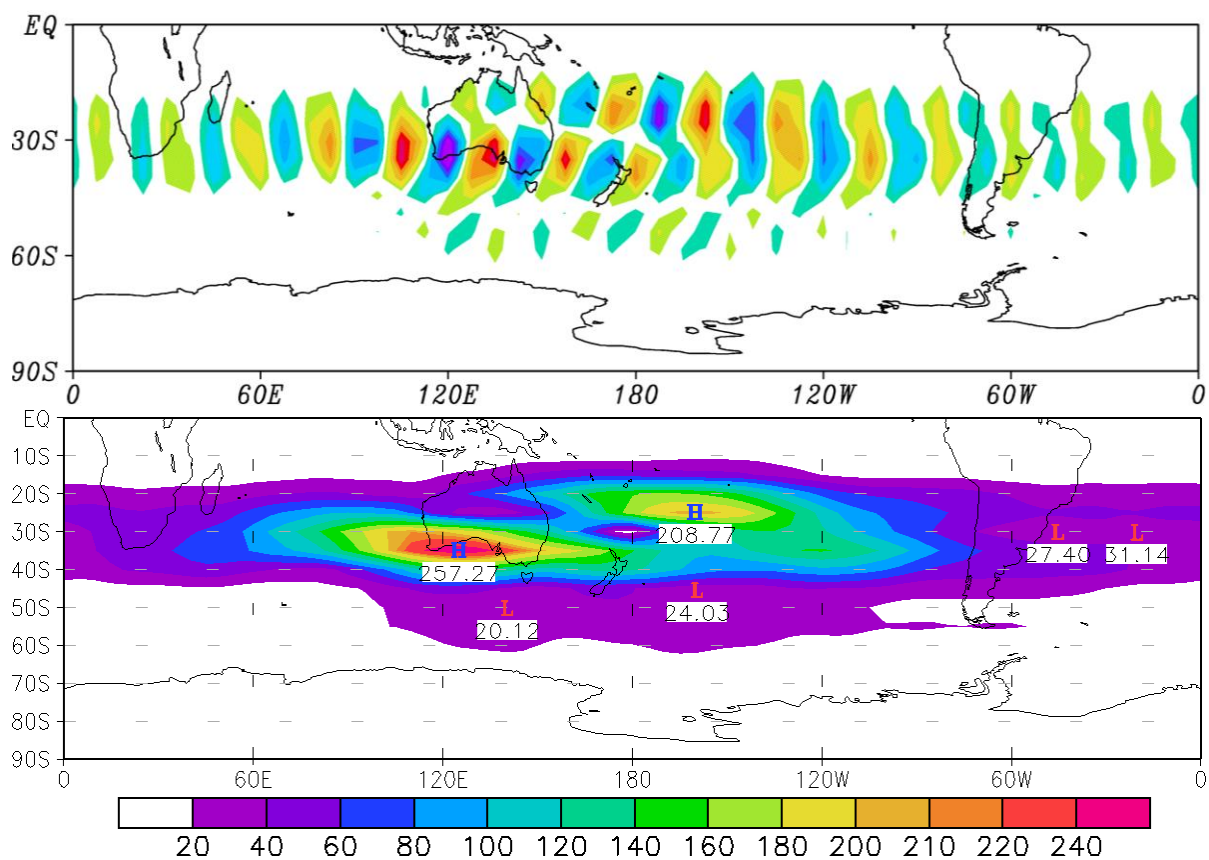


**Figure 1.1.1. The fastest growing July storm mode, mode 1, for the period 1949-1968. Shown in top panel are the 300 hPa troughs (blue) and ridges (red) of the streamfunction at a particular instance and in bottom panel the corresponding amplitude for the storm track. Units are relative.**

The bottom panel of Figure 1.1.1 shows the storm track associated with this mode and indicates that its largest impact (red shading) is over south-western Australia. By contrast, in the latter periods 1975-1994 and 1997-2006, the dominant SH storm mode has a different horizontal structure. In particular, this weather mode effectively

bypasses SWWA and has maximum impact in the central south Pacific (not shown). There are, however, other subdominant weather modes (Figure 1.1.2), with a similar structure and frequency to the dominant mode from the earlier period, but their growth rates have been greatly reduced affecting their ability to develop. This is consistent with the observed continuing reduction in rainfall over southern Australia, and in particular, SWWA. Figure 1.1.2 shows the corresponding storm track modes for the period 1975-1994 (mode 9) and 1997-2006 (mode 12).

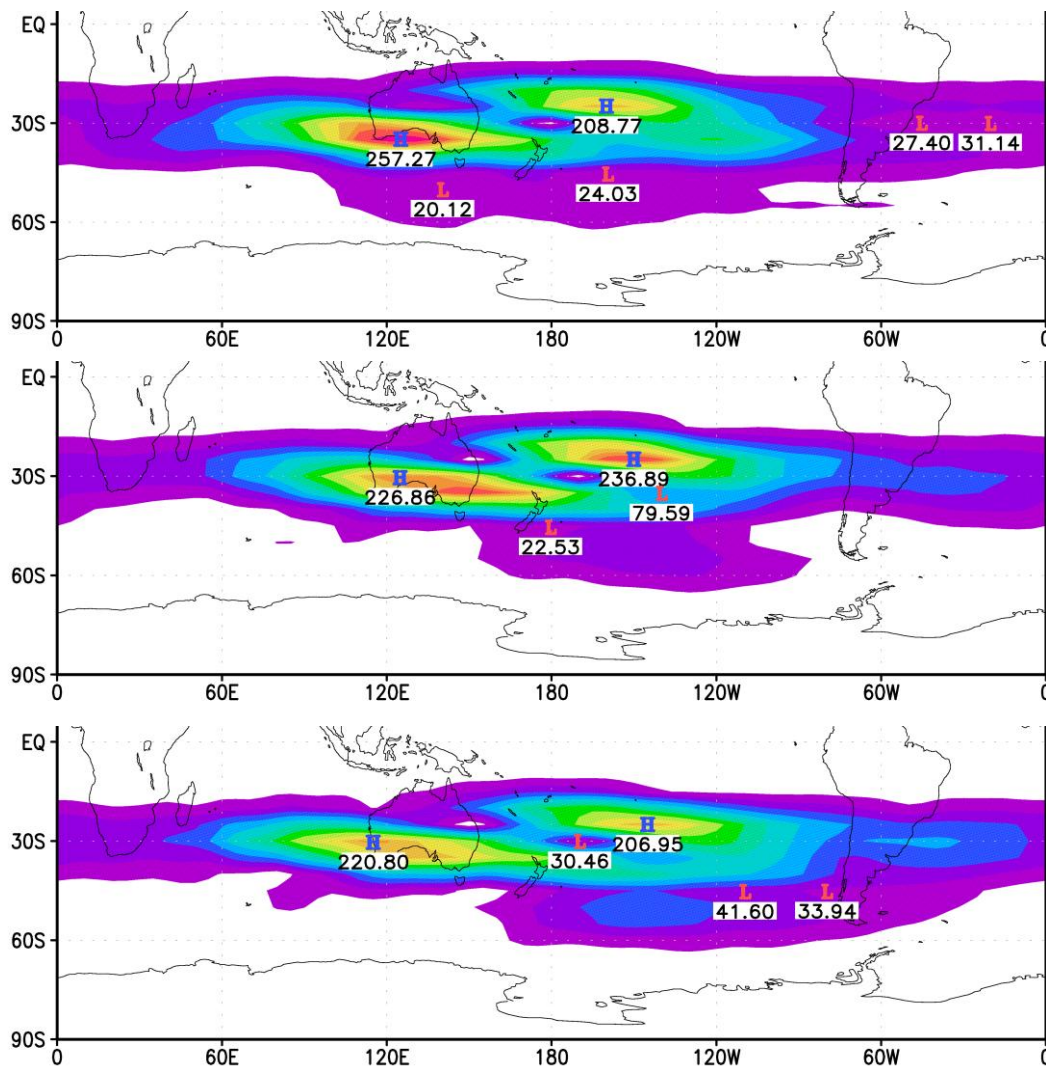


**Figure 1.1.2. Amplitude of the fastest growing July storm mode, for the period 1949-1968 (top), 1975-1994 (middle) and 1997-2006 (bottom), affecting SWWA. These correspond to modes 1, 9 and 12 respectively for each period.**

**Table 1 . Properties of leading storm track modes crossing southern Australia**

Basic State	Mode	Correlation with Mode 1	Growth Rate, $\omega_i$	Change in $\omega_i$
1949-68 NCEP	1	1.0000	0.423 day <sup>-1</sup>	0.0%
1975-94 NCEP	9	0.9148	0.282 day <sup>-1</sup>	-33.5%
1997-2006 NCEP	12	0.8960	0.266 day <sup>-1</sup>	-37.1%

We note from Table 1 that compared with the results for 1949-1968 there has been a reduction in the growth rate during the periods 1975-1994 (by 33.5%) and 1997-2006 (by 37.1%). The reductions in growth rates of the leading storm track modes in later periods, described above, also occurs for averages taken over the leading 10 or 20 modes that cross Australia, indicating that it is a robust result.

For May we have calculated the average root mean square (RMS) amplitude of the 20 fastest growing storm track modes (with each mode normalised to having the same RMS amplitude) for each of the three periods 1949-68, 1975-94 and 1997-2006. The reduction in the average growth rate of the 20 fastest growing storm track modes is only about 10% in the latter periods. However, there are dramatic changes in their structures. The results are shown in Figure 1.1.3. We note that for the early period 1949-68 the principal storm track is at the latitudes of the subtropical jet; it crosses Australia and has its maximum downstream. In contrast, for 1975-94, the subtropical storm track is reduced in amplitude and the polar storm track is strengthened. This reduction of the strength of the storm track crossing Australia continues in the period 1997-2006. The RMS associated divergence field across Australia is also reduced correspondingly in the latter periods, as shown in Figure 1.1.4, and this explains the observed reduction in rainfall over SWWA and southern Australia that has occurred in the latter part of the 20<sup>th</sup> century.

## **Conclusions**

There has been approximately a 20% reduction in autumn and winter SWWA rainfall, and a 17% reduction in peak July jet stream strength. Similar changes in the circulation have occurred in May. In July there has been about 30% reduction in growth rates of leading SH storm track modes crossing Australia since the mid 1970s. These changes have continued and spread to south-east Australia during the period 1997-2006. The structures of leading July storm track modes crossing Australia are very similar during 20<sup>th</sup> century. A primary cause of the rainfall reduction over SWWA since 1975 is the reduction in the intensity of storm development and the southward deflection of some storms. In May the strength of the subtropical storm track crossing Australia has decreased while the polar storm track has increased. This is the principal reason for the observed and continuing reduction in rainfall over SWWA and southern Australia during autumn.

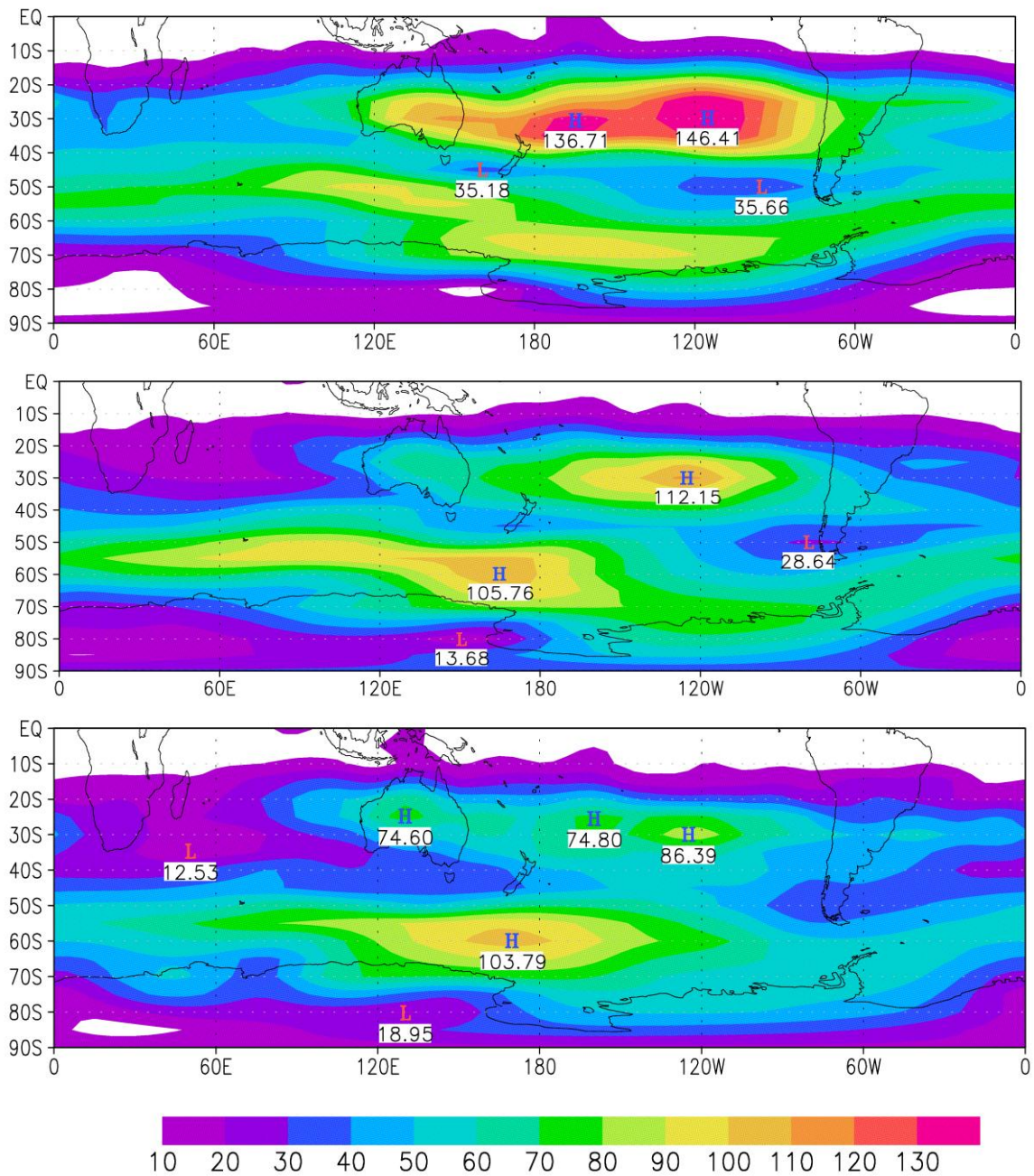


**Figure 1.1.3. RMS 300 hPa streamfunction averaged over 20 fastest growing May storm track modes for 1949-68 (top panel), 1975-94 (middle panel) and 1997-2006 (bottom panel).**

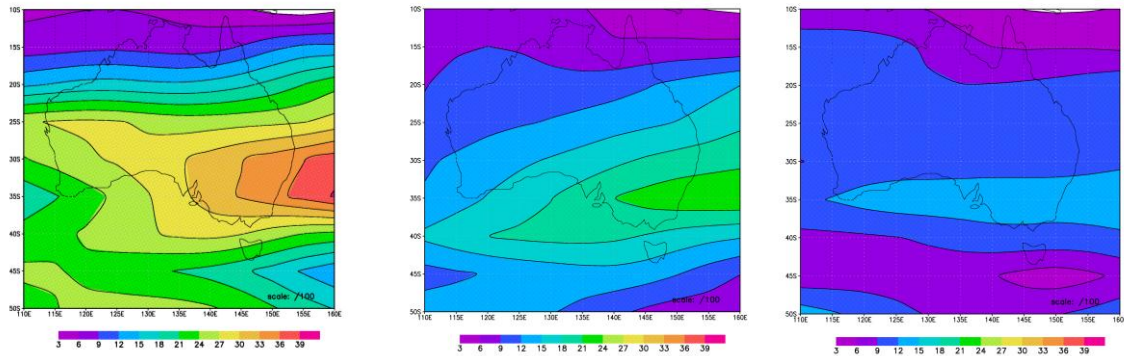


**Figure 1.1.4. RMS 700hPa divergence averaged over 20 fastest growing May storm track modes for 1949-68 (left panel), 1975-94 (middle panel) and 1997-2006 (right panel).**

## References

- Bates, B.C., Hope, P., Ryan, B. et al. (2008), Key findings from the Indian Ocean Climate Initiative and their impact on policy development in Australia. *Clim. Dyn.*, 89, 339-354.
- Cai, W. and Cowan, T. (2008), Dynamics of late autumn rainfall reduction over southeastern Australia. *Geophys. Res. Lett.*, 35, L09708, 5pp.
- Frederiksen, J. S. and Frederiksen, C.S., (2005), Decadal Changes in Southern Hemisphere Winter Cyclogenesis . *CSIRO Marine and Atmospheric Research Paper No. 002*, 35pp.
- Frederiksen, J.S. and Frederiksen, C.S. (2007), Inter-decadal changes in Southern Hemisphere winter storm track modes. *Tellus*, 59 A, 559-617.
- Nicholls, N. (2007), *Detecting, Understanding and Attributing Climate Change*. Australian Greenhouse Office Publication, 26pp.
- Ummenhofer, C.C., Sen Gupta, C., Pook, M.J. et al. (2008), Anomalous rainfall over southwest Western Australia forced by Indian Ocean sea surface temperatures. *J. Climate*, 21, 5113-5134.

## LIST OF TABLES

Table 1	Properties of leading storm track modes crossing southern Australia... 8	
Table 2	Properties of model leading storm track modes crossing southern Australia.....	24

## LIST OF FIGURES

Figure 1.1.1.	The fastest growing July storm mode, mode 1, for the period 1949-1968. Shown in top panel are the 300 hPa troughs (blue) and ridges (red) of the streamfunction at a particular instance and in bottom panel the corresponding amplitude for the storm track. Units are relative. ....	6
Figure 1.1.2.	Amplitude of the fastest growing July storm mode, for the period 1949-1968 (top), 1975-1994 (middle) and 1997-2006 (bottom), affecting SWWA. These correspond to modes 1, 9 and 12 respectively for each period. ....	7
Figure 1.1.3.	RMS 300 hPa streamfunction averaged over 20 fastest growing May storm track modes for 1949-68 (top panel), 1975-94 (middle panel) and 1997-2006 (bottom panel).....	10
Figure 1.1.4.	RMS 700hPa divergence averaged over 20 fastest growing May storm track modes for 1949-68 (left panel), 1975-94 (middle panel) and 1997-2006 (right panel).....	11
Figure 1.1.5.	300hPa zonal velocity ( $\text{ms}^{-1}$ ) from NCEP reanalysis for July (a) 1949-68, (b) 1975-1994 and (c) the difference (b)-(a).....	16
Figure 1.1.6.	Anomaly pattern correlation between the NCEP 300hPa zonal velocity difference (Figure 1 (c)) and model difference for (i) (1975-94)-(1949-68) (black bar), (ii) (1980-99) – PICNTRL (green bar), (iii) (1980-99) – PICNTRL_20 (blue bar) and (iv) (1980-99) – PICNTRL_40 (red bar). ...	17
Figure 1.1.7.	Phillips instability criterion ( $\text{ms}^{-1}$ ) from NCEP reanalysis for July (a) 1949-68, (b) 1975-1994 and (c) the difference (b)-(a). ....	19
Figure 1.1.8.	Anomaly pattern correlation between the NCEP Phillips criterion difference (Figure 3 (c)) and model Phillips criterion difference for (i) (1975-94)-(1949-68) (black bar), (ii) (1980-99) – PICNTRL (green bar), (iii) (1980-99) – PICNTRL_20 (blue bar) and (iv) (1980-99) – PICNTRL_40 (red bar). ....	20
Figure 1.1.9.	Differences in Phillips criterion ( $\text{ms}^{-1}$ ) for (i) (1975-94) – (1949-68), (ii) (1980-99) – PICNTRL, (iii) (1980-99) - PICNTRL_20 and (iv) (1980-99) – PICNTRL_40, for <i>miroc3_2_medres</i> . ....	21
Figure 1.1.10.	Differences in Phillips criterion ( $\text{ms}^{-1}$ ) for (1980-99) – PICNTRL and projected changes for (i) SRESB1 – PICNTRL, (ii) SRESA1B – PICNTRL and (iii) SRESA2 – PICNTRL, for <i>miroc3_2_medres</i> . ....	22

## **MILESTONE 1.1.2: REPORT ON SIMULATED CHANGES IN MEAN SH CLIMATE AND TRANSIENTS UNDER OBSERVED ANTHROPOGENIC FORCING**

### **Background**

#### *Summary*

The performance of coupled models to simulate twentieth century winter circulation changes throughout the southern hemisphere, and particularly over Australia has been examined. Changes include a decrease in the vertical mean meridional temperature gradient and in the peak upper tropospheric jet-stream zonal winds throughout most of the southern hemisphere, but especially upstream and over Australia. These and other circulation changes, including changes in the Hadley circulation, and trends in the Southern Annular Mode, affect winter rainfall over SWWA and southern Australia. Here, we examine the response of many of the Coupled Model Intercomparison Project 3 (CMIP3) climate models to observed anthropogenic forcing, including increasing greenhouse gases, from pre-industrial to the end of the twentieth century.

Our interest here is on changes in the atmospheric circulation that affect wintertime storm development, and for that reason we focus on two diagnostics that can be used to evaluate the climate models in this regard. Thus, our focus is on the ability to simulate (a) the reduction in the strength of the wintertime subtropical 300hPa zonal wind upstream and over southern Australia, and a strengthening in the zonal wind further south, and (b) a reduction in the baroclinic instability, related to the vertical wind shear, of the subtropical SH circulation.

The CMIP3 models display quite disparate abilities to simulate these two diagnostics. While the majority is able to simulate the former ((a)), especially when using the pre-industrial simulations, only about a third of the models capture the changes in the latter ((b)). Our analysis also suggests that there is a component of decadal variability in the model results that is dependent on the base period chosen in the pre-industrial runs.

There are a number of models that consistently simulate changes in the two diagnostics that are in general agreement with results from the NCEP reanalysis.

Projected changes in baroclinic instability from these models suggest that further large reductions in baroclinic instability are possible under SRESB1, SRESA1B and SRESA2 scenarios, especially over the Australian region. By implication, this suggests further reductions in the growth rates of SH storm track modes and further reductions in rainfall, over southern Australia.

We have also examined the ability of a number of climate models with anthropogenic forcing including increasing greenhouse gas concentrations to replicate the changes in transient weather systems during the 20th century. Here, we focus on Australian models including the CSIRO Mark 3.0 and 3.5 coupled models and the ACCESS atmospheric model with prescribed SSTs; we also consider the UKMO HadGem1 coupled model that has a similar atmospheric component to the ACCESS model. The coupled models are not able to capture the storm track changes. However, the leading storm track mode crossing Australia from the ACCESS model simulations with prescribed SSTs has a structure that is remarkably similar to those based on July reanalyses and has reasonably good growth rate.

### *Introduction*

A number of studies have recently shown that the early to mid-1970s was a time of major shift in the structure of the large-scale circulation of both the northern and southern hemispheres (see for example Frederiksen and Frederiksen, 2005, 2007, for overview). Over southern Australia there was a concurrent, dramatic and continuing reduction in the winter rainfall (see for example Nicholls, 2007, and Bates et al. 2008, for overview). Very large reductions (~20%) in winter rainfall occurred first in the southwest of Western Australia (SWWA).

Most noticeable among the large-scale circulation changes was the decrease in the vertical mean meridional temperature gradient and in the peak upper tropospheric jet-stream zonal winds throughout most of the southern hemisphere, but in particular upstream and over Australia. These and other circulation changes, including changes in the Hadley circulation, and trends in the Southern Annular Mode, have been shown by the principal investigators to affect winter rainfall over SWWA and southern Australia.

Here, we examine the response of the CMIP3 climate models (Meehl et al., 2007) to observed natural and anthropogenic forcing, including increasing greenhouse gases, from pre-industrial to the end of the twentieth century. The extent, to which the models show similar atmospheric winter circulation changes, as seen in Frederiksen and Frederiksen (2007) for the reanalysis data, is discussed, as well as the implications of these results for climate change projections and attribution studies. We also examine storm track modes in the CSIRO Mark 3.0 and 3.5, ACCESS and UKMO HadGem1 climate models.

## **Technical Details**

### *Changes in SH Wintertime Circulation*

Frederiksen and Frederiksen (2007) found that there were quite large changes in the thermal structure and circulation in the Southern Hemisphere (SH) circulation between the periods 1949-1968 and 1975-1994. In particular, there was reduction in the strength of the subtropical 300hPa zonal wind upstream and over southern Australia, and extending over much of the hemisphere. Near 45-50°S, there was an increase in zonal wind. Also, they found a reduction in the baroclinic instability, as measured by a generalization of the Phillips (1954) criterion, of between 25-30% upstream and over SWWA. Because our interest here is on changes in the atmospheric circulation that affect cyclogenesis, these are two good diagnostics to use to evaluate the climate models. They are also very much related to other changes discussed by Frederiksen and Frederiksen (2007), including a reduction in the mean atmospheric meridional temperature gradient, changes in the Hadley circulation, and trends in the Southern Annular Mode. Here, we will compare the model results with the NCEP reanalysis.

#### *(a) Changes in 300h Zonal Winds*

Figure 1.1.5 shows the NCEP 300hPa zonal velocity averaged over the periods 1949-1968 and 1975-1994, and their differences. The difference plot shows quite dramatic reductions near 30°S in the latter period of up to  $7\text{ms}^{-1}$ , and increases between  $5\text{-}6\text{ms}^{-1}$

further south near 50°S. This difference in the zonal wind structure is clearly hemispheric and unlikely to be the response to some local phenomenon. Of particular interest is the region 60°E - 150°E, 60°S - 15°S. Frederiksen and Frederiksen (2007) showed that this area is very much related to the genesis of the storms that affect southern Australia. In this area, there are reductions in the sub-tropical zonal velocity of up to 4.7ms<sup>-1</sup> with increases up to 5.6ms<sup>-1</sup> further south.

In Figure 1.1.6, we show for twenty two of the CMIP3 models (see Randall et al., 2007 and Meehl et al., 2007, for model nomenclature and description) the anomaly pattern correlation (APC), calculated over the domain (60° S to 15° S, 60°E - 150°E) between the NCEP difference in 300hPa zonal winds (Figure 1.1.5c) and similar differences calculated with model data in four different ways. The black bars in Figure 1.1.6 are the APCs with zonal wind differences calculated for models using the same two twenty year periods (1949-68 and 1975-94) as for the NCEP reanalysis (i.e. the 20C3M simulations, Meehl et al., 2007).

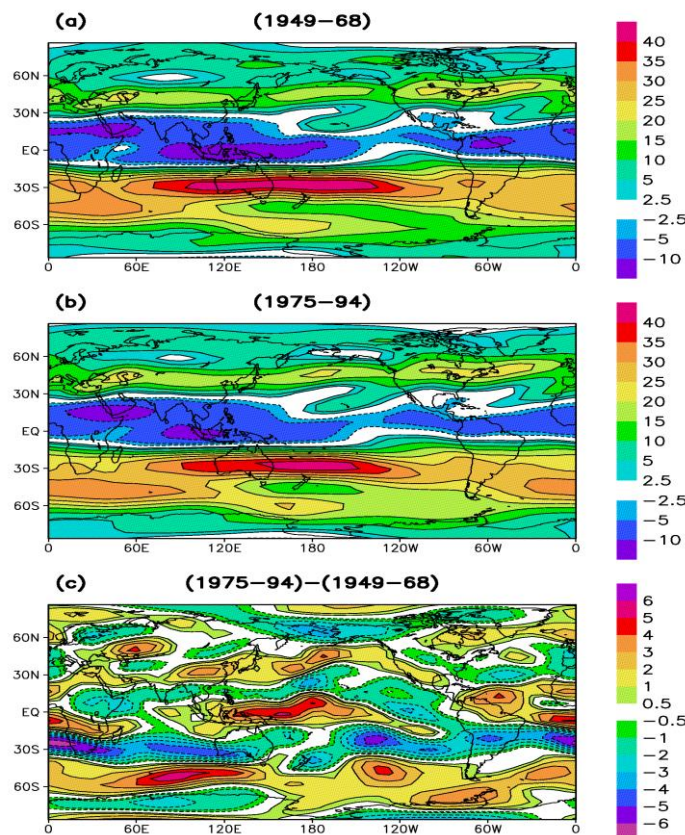


**Figure 1.1.5. 300hPa zonal velocity (ms<sup>-1</sup>) from NCEP reanalysis for July (a) 1949-68, (b) 1975-1994 and (c) the difference (b)-(a).**

However, because the timing of simulated changes in coupled models may not necessarily synchronize with the reanalyzed observations, we have also included APCs with model differences between pre-industrial control runs (i.e. the PICNTRL simulations, Meehl et al., 2007) and the (1980-1999) period of the 20C3M runs. This will give an indication of the impact of all the twentieth century greenhouse gas forcing. Also, we are interested in the sensitivity of our results to the base period chosen in the PICNTRL runs, and the possible influence of decadal variability on our results. For this reason, we have used three adjoining twenty year periods at the end of the PICNTRL runs, separated by twenty years. These are designated PICNTRL (green bar), PICNTRL\_20 (blue bar) and PICNTRL\_40 (red bar).

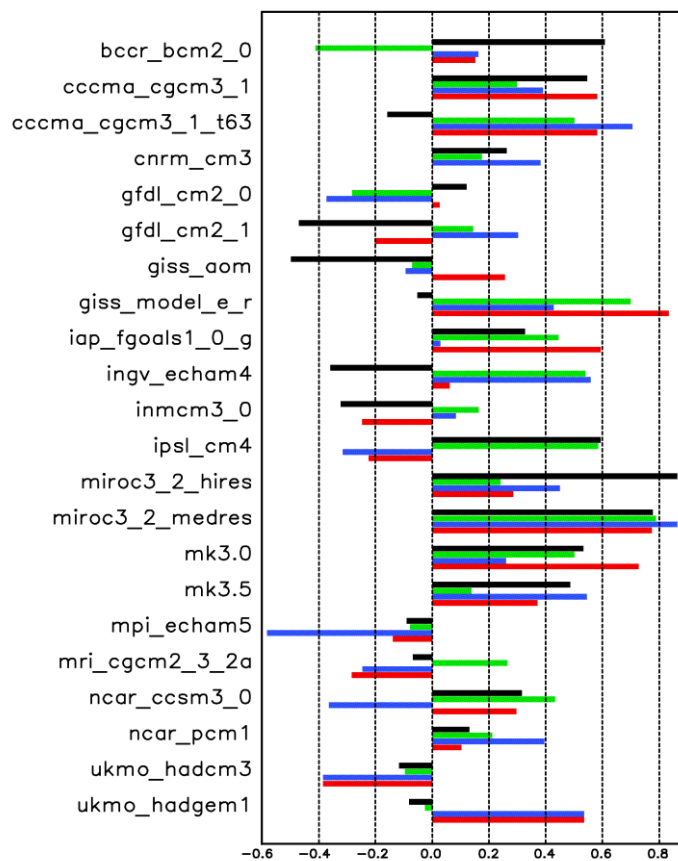


**Figure 1.1.6. Anomaly pattern correlation between the NCEP 300hPa zonal velocity difference (Figure 1 (c)) and model difference for (i) (1975-94)-(1949-68) (black bar), (ii) (1980-99) - PICNTRL (green bar), (iii) (1980-99) - PICNTRL\_20 (blue bar) and (iv) (1980-99) - PICNTRL\_40 (red bar).**

Figure 1.1.6 shows that the ability of models to reproduce the reanalysis changes during the same two twenty year periods is quite variable, with some models showing opposite sign in the zonal wind differences. When changes from pre-industrial simulations are taken into account, there is clear evidence of a component of decadal variability with the APCs showing some dependence on the base period. For some models, this is seen in the changing sign of the APC (e.g. *gfdl\_cm2\_1*), and for others in changes in the magnitude of the APC (e.g. *mk3.0*). Some models show quite large APC with the reanalysis results (e.g. *miroc3\_2\_medres*, *miroc3\_2\_hires* and *giss\_model\_e\_r*). A number of models show consistently positive APC in all four cases (e.g. *miroc3\_2\_medres*, *miroc3\_2\_hires* and *mk3.0*). Overall the majority of the models do simulate the changes in the zonal wind upstream and over southern Australia, especially in differences between the pre-industrial and end of the twentieth century simulations. The *miroc3\_2\_medres*, in particular, simulates the SH changes seen in Figure 1(c) remarkably well (not shown).

*(b) Changes in Baroclinic Instability*

The Phillips (1954) criterion, generalized for spherical geometry, is a simple diagnostic that provides a measure of incipient baroclinic instability and can be used to identify geographical regions of possible storm development (Frederiksen and Frederiksen, 1992). This criterion may be written as

$$(\bar{u}^{(300)} - \bar{u}^{(700)}) - u_c^s \geq 0. \quad (1)$$

Here,  $\bar{u}^{(300)}$  and  $\bar{u}^{(700)}$  represent the 300 hPa and 700 hPa zonal wind, and  $u_c^s$  the critical vertical wind shear for instability, that depends on latitude, (see Eqn. (3.1) of Frederiksen and Frederiksen, 1992) for a given climate. Near the equator, the left hand side of Eqn. (1) is always negative and therefore this criterion is mostly relevant for the development of extra-tropical storms.

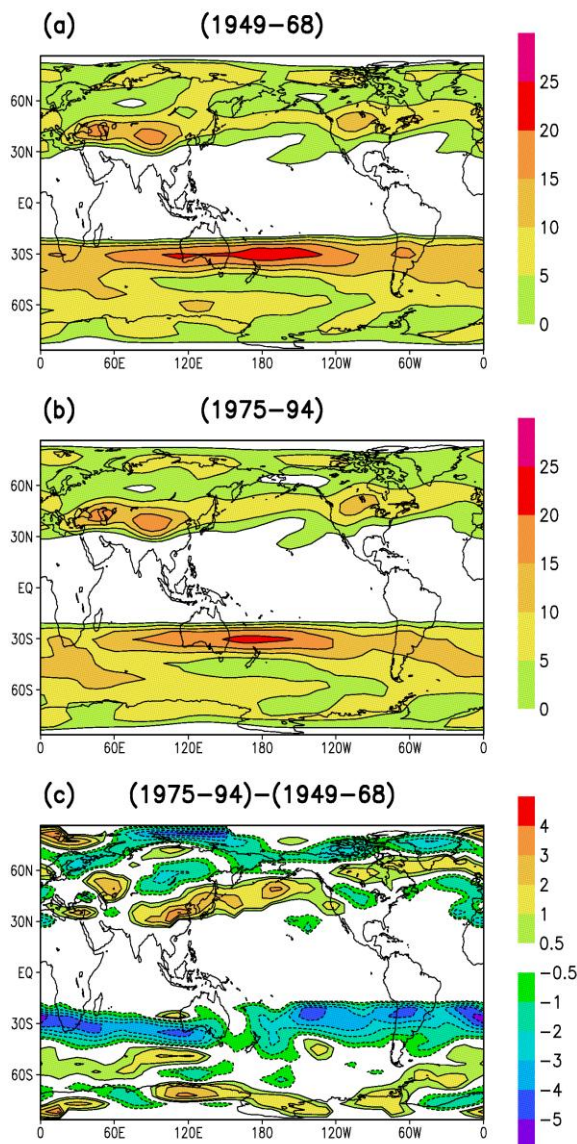


**Figure 1.1.7. Phillips instability criterion ( $\text{ms}^{-1}$ ) from NCEP reanalysis for July (a) 1949-68, (b) 1975-1994 and (c) the difference (b)-(a).**

In Figure 1.1.7, we show, for the NCEP reanalysis, regions where this baroclinic instability criterion is positive for the 1949-68 and 1975-94 basic states, and their difference respectively. For both July climates, these regions coincide with the subtropical jet and a maximum in the criterion occurs in the South Pacific near 30° S. The difference plot (Figure 1.1.7c) shows a reduction in the criterion in the latter period that extends across the whole hemisphere in a band centered near 30°S. As discussed in Frederiksen and Frederiksen (2007), this is associated with a reduction of storm development throughout this band and the reduction in growth rate of the SH storm track modes. Essentially, the SH has become less baroclinically unstable near 30° S in

the latter period compared with the former. In contrast, poleward of about 45° S there is an increase in baroclinic instability, especially south and upstream of Australia. Importantly, there is a reduction of about 4.5ms<sup>-1</sup> situated over SWWA.

Figure 1.1.8 shows the APCs, calculated for the region 60°E - 150°E, 45°S - 15°S, between the NCEP Phillips criterion difference (Figure 1.1.7(c)) and the model differences for the same four cases discussed in the previous section. For this diagnostic, there is much more variability in the models to simulate the reanalysis results. About a third of the models show a consistently negative APC in all four cases (e.g. *gfdl\_cm2\_1*, *giss\_aom*, *mpi\_echam5* etc.). For these models, there is an increase in baroclinic instability that would lead to an increase in growth of the storm modes. However, about a third of the models show a consistently positive APC (e.g. *miroc3\_2\_medres*, *giss\_model\_e\_r*, *ncar\_ccsm3\_0* etc.). Again, as for the zonal velocity, there is evidence of a component of decadal variability in the model results.

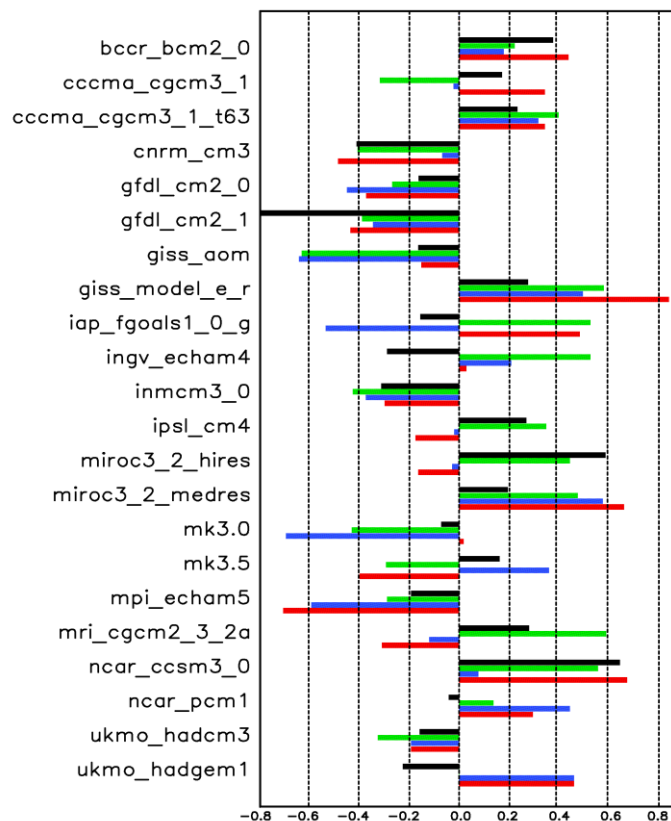


**Figure 1.1.8. Anomaly pattern correlation between the NCEP Phillips criterion difference (Figure 3 (c)) and model Phillips criterion difference for (i) (1975-94)-(1949-68) (black bar), (ii) (1980-99) – PICNTRL (green bar), (iii) (1980-99) – PICNTRL\_20 (blue bar) and (iv) (1980-99) – PICNTRL\_40 (red bar).**

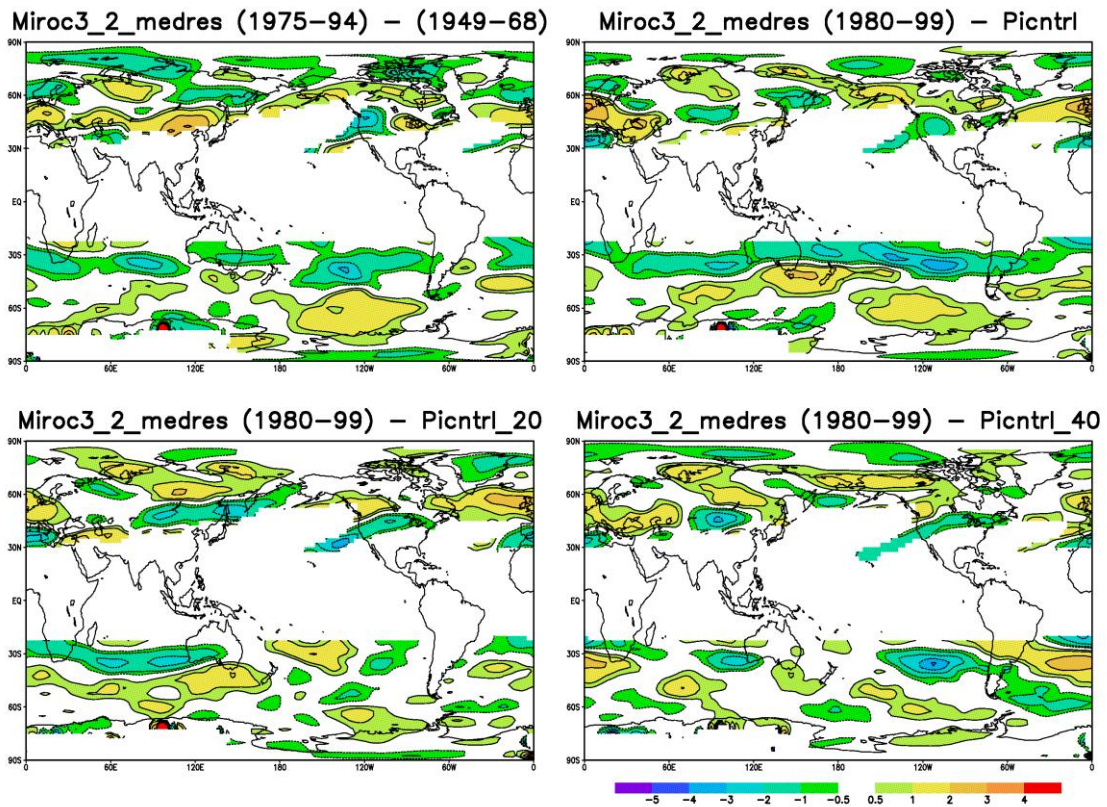


**Figure 1.1.9. Differences in Phillips criterion ( $\text{ms}^{-1}$ ) for (i) (1975-94) – (1949-68), (ii) (1980-99) – PICNTRL, (iii) (1980-99) - PICNTRL\_20 and (iv) (1980-99) – PICNTRL\_40, for *miroc3\_2\_medres*.**

The *miroc3\_2\_medres* model agrees fairly consistently with the NCEP reanalysis changes seen in both diagnostics. For example, Figure 1.1.9 shows the Phillips criterion differences for this model in all four cases. The difference between the (1980-1999) period and the last 20 years of the PICNTRL run is remarkably similar to the NCEP changes (Figure 3(c)) throughout the subtropical SH.

*(c) Future Projected Changes in Baroclinic Instability*

Here, we shall discuss projections of possible changes in baroclinic instability under three different climate change scenarios using the *miroc3\_2\_medres* model. The three scenarios we will consider are the Special Report on Emission Scenarios (SRES) B1, A1B and A2 (see, for example, Meehl et al., 2007). These involve low, medium and high  $\text{CO}_2$  concentrations of 550ppm, 700ppm and 820ppm, respectively, by 2100. Figure 6 shows the changes in Phillips criterion for (1980-1999) – PICNTRL, SRESB1 – PICNTRL, SRESA1B – PICNTRL and SRESA2 – PICNTRL, using this model. As the  $\text{CO}_2$  concentrations increases, there are progressively larger reductions in the subtropical baroclinic instability, especially over the Australian region. In the

SRESA1B and SRESA2 scenarios, these differences are about twice those seen in the model for the twentieth century run. This suggests further reductions in the growth rate of the SH storm track modes and a worsening of drought conditions over southern Australian. However, the exact nature of the changes in growth rates and three-dimensional structures of the cyclogenesis modes requires a full three dimensional instability analysis to be conducted, and we have plans to do this in a future studies.

We have also looked at projected changes in other models that show good correspondence with the reanalysis results (e.g. the *giss\_model\_e\_r* and *ncar\_ccsm3\_0* models) and they confirm the results from the *miroc3\_2\_medres* model.

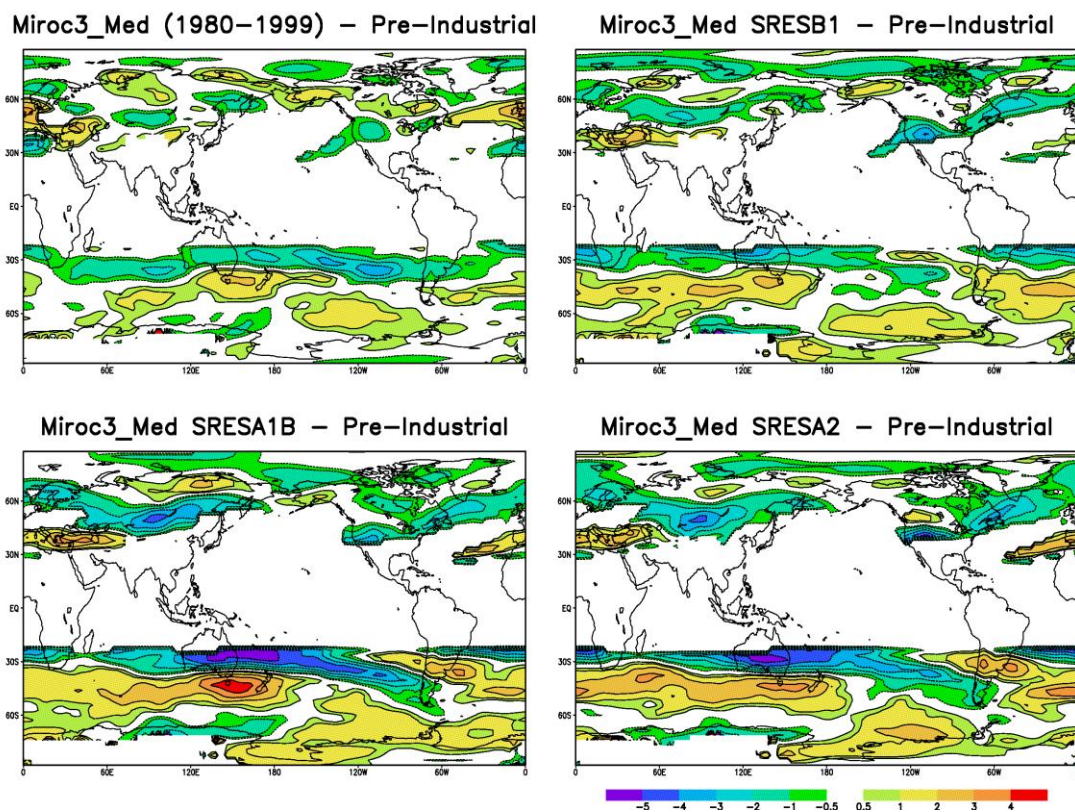


**Figure 1.1.10. Differences in Phillips criterion ( $\text{ms}^{-1}$ ) for (1980-99) – PICNTRL and projected changes for (i) SRESB1 – PICNTRL, (ii) SRESA1B – PICNTRL and (iii) SRESA2 – PICNTRL, for *miroc3\_2\_medres*.**

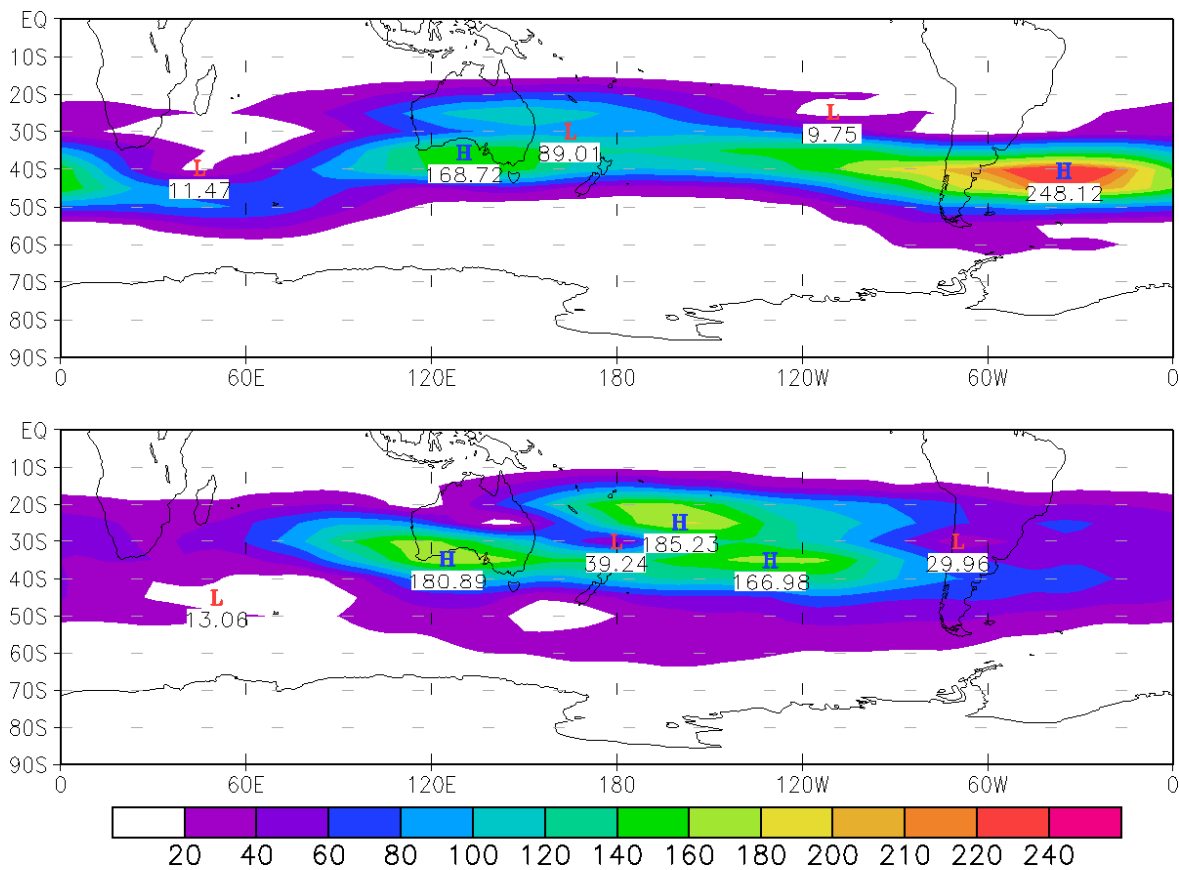


**Figure 1.1.11.** As in bottom panel of Figure 1 for July mode 9 for CSIRO Mark 3.0 model run with pre-industrial forcing (top panel) and July mode 2 for 1980-2000 with ACCESS model (bottom panel).

*Storm Track Modes from Climate Models*

We have examined July storm track modes in Australian climate models including the CSIRO Mark 3.0 and 3.5 coupled ocean-atmosphere models and the ACCESS atmospheric model with prescribed SSTs. We have also considered the HadGem1 coupled model that has a similar atmospheric component to the ACCESS model. The top panel of Figure 1.1.11 shows July mode 9, the leading storm track mode crossing southern Australia, using data from the CSIRO Mark 3.0 coupled model run with pre-industrial forcing. We note that the peak of the leading storm track mode occurs over the southern Atlantic rather than over southern Australia; the same failing occurs with other fast growing storm track modes. As seen from Table 2, the correlation with mode 1 for 1949-1968 is poor at 0.54 and its growth rate is too low.

Basic State	Mode	Correlation with Mode 1	Growth Rate, $\omega_i$	Change in $\omega_i$
1949-68 NCEP	1	1.0000	0.423 day <sup>-1</sup>	0.0%
Pre Indust CSIRO 3.0	4	0.5435	0.293 day <sup>-1</sup>	-30.7%
Pre Indust HadGem1	11	0.5770	0.336 day <sup>-1</sup>	-20.6%
1980-99 HadGem1	2	0.7995	0.481 day <sup>-1</sup>	+13.7%
1980-99 ACCESS	2	0.9013	0.367 day <sup>-1</sup>	-13.3%

**Table 2 Properties of model leading storm track modes crossing southern Australia**

These deficiencies also apply to the CSIRO Mark 3.5 model. For the HadGem1 coupled model with pre-industrial forcing the structure of the storm track is again poor with maximum amplitude over the south-west Pacific. Again, correlation with mode 1 for 1949-1968 is low at 0.57 and its growth rate is low.

The bottom panel of Figure 1.1.11 shows July mode 2, the fastest growing storm track mode crossing southern Australia in the ACCESS atmospheric model with prescribed SSTs for the period 1980-1999. It has a similar structure to the leading storm track modes during the second half of the twentieth century (Figures 1 and 2). From Table 2 we note that the correlation with mode 1 for 1949-1968 is 0.9, which is similar to the results for the reanalyses for the periods 1975-1994 and 1997-2006. We also see that its growth rate is reduced compared with the period 1949-1968 in the reanalyses but somewhat larger than for the later periods. Table 1 also shows the results for the HadGem1 coupled model for the period 1980-1999. We see that the correlation with mode 1 for 1949-1968 reanalyses is less than for the ACCESS model but still quite reasonable at 0.8. However, the growth rate is much too large compared with the reanalyses for the twentieth century. We plan to analyse the CMIP3 models in the near future.

## Conclusions

The ability of the CMIP3 models to simulate a wintertime reduction in the baroclinic instability of the SH subtropics and the 300hPa zonal winds near 30° S, is quite variable. About a third of the models are able to simulate the former, and the majority the latter, especially when compared with pre-industrial conditions. It is clear from the

results presented here that there is a component of decadal variability in the model results that is dependent on the base period chosen in the pre-industrial runs. This means that attribution and projection of atmospheric circulation changes will involve the disentanglement of decadal variability and anthropogenic climate change.

There are a number of models that consistently, in all the four cases considered here, simulate changes in our two diagnostics that are in good general agreement with results from the NCEP reanalysis. Projected changes in baroclinic instability from these models suggest that further large reductions in baroclinic instability are possible under SRESB1, SRESA1B and SRESA2 scenarios, especially over the Australian region. By implication, this suggests further reductions in the growth rates of SH cyclogenesis modes, and further reductions in rainfall over southern Australia.

Many climate models have difficulty in capturing the detailed structure of the Southern Hemisphere circulation and transient weather systems and their changes during the 20<sup>th</sup> century. A summary of the performance of the CSIRO, UKMO and ACCESS models has been presented. The structure of the leading SH winter storm track mode crossing Australia, using data from the ACCESS Atmospheric Model Intercomparison Project (AMIP) run, is in very good agreement with results from reanalysed observations and its growth rate is reasonable.

The analysis conducted here provides a convenient means of evaluating the CMIP3 models as far as their ability to simulate changes in the atmospheric circulation that are relevant for studying changes in the climatological storm tracks. In future studies, we plan to conduct much more comprehensive three-dimensional studies with the “better” models to determine projected changes in the actual growth rates and three-dimensional structure of the storm track modes. From this we hope to describe the expected impact on southern Australian rainfall.

## References

- Bates, B.C., P. Hope and B. Ryan (2008), Key findings from the Indian Ocean Climate Initiative and their impact on policy development in Australia, *Climatic Change*, 89, 339-354.
- Frederiksen, C.S. and J.S. Frederiksen (1992), Northern hemisphere storm tracks and teleconnection patterns in primitive equation and quasigeostrophic models, *J. Atmos. Sci.*, 49, 1443-1458.
- Frederiksen, J. S. and C.S. Frederiksen, (2005), Decadal Changes in Southern Hemisphere Winter Cyclogenesis. *CSIRO Marine and Atmospheric Research Paper* No. 002, 35pps.
- Frederiksen, J.S. and C.S. Frederiksen (2007), Interdecadal changes in southern hemisphere winter storm track modes, *Tellus*, 59A, 599-617.
- Meehl, G.A. et al. (2007), The WCRP CMIP3 multimodel dataset: A new era in climate change research, *Bull. Amer. Meteor. Soc.*, 88, 1383-1394, doi:10.1175/BAMS-88-9-1383.
- Nicholls, N. (2007), Detecting, understanding and attributing climate change, *Australian Greenhouse Office Publication*, 26pp.
- Phillips, N.A. (1954), Energy transformations and meridional circulations associated with simple baroclinic waves in a two-level, quasi-geostrophic model. *Tellus*, 6, 273-286.
- Randall, D.A., et al. (2007), Climate models and their evaluation, in *Climate Change 2007: The Physical Science Basis. Contribution of Working Group I to the Fourth Assessment Report of the Intergovernmental Panel on Climate Change*, edited by S. Solomon et al., pp. 589-662, Cambridge Univ. Press, Cambridge, U. K.

## Publications

- Frederiksen, C.S., J.S. Frederiksen, J.M. Sisson, and S.L. Osbrough, 2009: *Australian Winter Circulation and Rainfall Changes and Projections*. *Journal of Climate Change Strategies and Management*. (submitted).
- Frederiksen, J.S., C.S. Frederiksen, S.L. Osbrough and J.M. Sisson, 2009: *Causes of changing Southern Hemispheric weather systems*. GH2009 book, CSIRO publication. (in press)

Frederiksen, J.S., C.S. Frederiksen and S.L. Osbrough, 2009: *Modelling of changes in Southern Hemisphere weather systems during the 20<sup>th</sup> century*. 18<sup>th</sup> World IMACS/MODSIM Congress, Cairns, Australia, 13-17 July, 2009. (<http://www.mssanz.org.au>)

Frederiksen, C.S., J.S. Frederiksen and J.M. Sisson, 2009: *Simulations of twentieth century atmospheric circulation changes over Australia*. 18<sup>th</sup> World IMACS/MODSIM Congress, Cairns, Australia, 13-17 July, 2009. (<http://www.mssanz.org.au>)

Frederiksen, J.S., C.S. Frederiksen and S.L. Osbrough, 2009: *Changes in Southern Hemisphere storm tracks during the twentieth century*. A Changing Climate: Western Australia in focus, presenters' abstract papers. The University of Western Australia publication, 46pps. 10-1